Mühendislik Bilimleri ve Tasarım Dergisi
7(4), 796 – 802, 2019
e-ISSN: 1308-6693

Journal of Engineering Sciences and Design
DOI: 10.21923/jesd.474834

Araştırma Makalesi Research Article

EFFECT OF FRIT CONTENT IN THE SILVER CURRENT COLLECTOR INKS ON THE ELECTROCHEMICAL PERFORMANCE OF SOLID OXIDE FUEL CELL CATHODES

Emrah DEMİRKAL[1], Aligül BÜYÜKAKSOY*[1,2]

[1] Department of Materials Science and Engineering, Faculty of Engineering, Gebze Technical University, Kocaeli, Turkey
[2] Institute of Nanotechnology, Gebze Technical University, Kocaeli, Turkey

Keywords
Solid Oxide Fuel Cells,
Current Collectors,
Silver,
Impedance Spectroscopy,
Cathode.

Abstract

Silver (Ag) inks are often used as precursors to form current collector layers on the intermediate-temperature solid oxide fuel cell (SOFC) cathodes. It has been common practice to add glassy phase (frit) particles into the Ag inks to achieve good adhesion between the current collector and the cathode layers upon firing. However, insufficient attention has been given to the effects of frit content on the microstructure and the current collecting properties of Ag layers. This study presents the effect of frit addition on the measured electrochemical performance of $La_{0.6}Sr_{0.4}FeO_3$ (LSF) thin film cathodes. Microstructural analyses reveal that frit addition significantly densifies the Ag current collector layer. The glassy phase replacing Ag reduces the contact area between the Ag particles and the LSF thin film cathode, resulting in increased ohmic resistances. The glassy phase also seals the electrocatalytic surface of the LSF thin film, thus enhancing the cathode polarization resistances. Electrochemical impedance spectroscopy measurements on symmetrical half-cells reveal that ohmic resistances matching the resistivity of the yttria stabilized zirconia electrolyte (YSZ) and acceptable cathode polarization resistances (e.g., 0.5 Ωcm^2 at 700°C in air) can be obtained when frit-free Ag current collector inks are used.

GÜMÜŞ AKIM TOPLAYICI MÜREKKEPLERİNDE FRİT BULUNMASININ KATI OKSİT YAKIT HÜCRESİ KATOTLARININ ELEKTROKİMYASAL PERFORMANSINA ETKİSİ

Anahtar Kelimeler
Katı Oksit Yakıt Hücreleri,
Akım Toplayıcı,
Gümüş,
Empedans Spektroskopisi,
Katot.

Öz

Gümüş (Ag) içeren asıltılar (mürekkepler) orta sıcaklıklarda çalışan katı oksit yakıt hücresi (KOYH) katotları üzerine sıklıkla akım toplayıcı olarak uygulanırlar. Bu mürekkeplere camsı faz (frit) parçacıklarının ısıl işlem sonrasında altlığa iyi yapışma sağlanması amacıyla eklenmesi geleneksel olarak uygulanagelmiştir. Fakat bu parçacıkların Ag mürekkeplerine eklenmelerinin akım toplayıcı mikroyapısı ve performansı üzerindeki etkileri net olarak tespit edilmemiştir. Bu çalışmada gümüş mürekkeplerine frit eklenmesinin $La_{0.6}Sr_{0.4}FeO_3$ (LSF) ince film katotlarının elektrokimyasal performansına etkisi sunulmaktadır. Mikroyapısal analizler frit etkisinin Ag akım toplayıcı katmanını yoğunlaştırdığını göstermektedir. Ag yerine eklenen camsı faz Ag /LSF ince film katot arayüzey alanını azaltmakta ve yüksek ohmik dirence sebep olmaktadır. Camsı faz ayrıca LSF yüzeyini mühürlemekte, böylece yüksek polarizasyon dirençlerine yol açmaktadır. Simetrik yarı-hücreler üzerinde gerçekleştirilen elektrokimyasal empedans spektroskopisi ölçümleri frit içermeyen Ag mürekkepleri kullanıldığında itriya katkılı zirkonya elektrolitin özdirenci ile örtüşen ohmik dirençler ve kabul edilebilir katot polarizasyon dirençlerinin (örn., 700 °C ve durağan hava ortamında 0.5 Ωcm^2) elde edilebildiğini göstermektedir.

---

*İlgili yazar / Corresponding author: aligul@gtu.edu.tr, +90-262-605-2662

Alıntı / Cite

Emrah D., Aligül B., (2019). Effect of Frit Content in the Silver Current Collector Inks on the Electrochemical Performance of Solid Oxide Fuel Cell Cathodes, Journal of Engineering Sciences and Design, 7(4), 796-802.

Yazar Kimliği / Author ID (ORCID Number)	**Makale Süreci / Article Process**	
E. Demirkal, 0000-0001-7607-2009 A. Büyükaksoy, 0000-0003-2227-8938	**Başvuru Tarihi /Submission Date**	25.10.2018
	Revizyon Tarihi / Revision Date	20.05.2019
	Kabul Tarihi / Accepted Date	27.05.2019
	Yayım Tarihi / Published Date	19.12.2019

1. Introduction

In pursuit of solid oxide fuel cells (SOFCs) with higher power densities, there has especially been an intensive effort to develop cathode materials with new chemistries and microstructures (Lyskov et al., 2018; Tatko et al., 2015; Li et al., 2014). To evaluate the performance of the developed cathode materials in the laboratory scale, electrochemical testing using single button cell or symmetrical half-cell configurations has been the widely adopted approach (Chen et al., 2015).

When performing electrochemical testing of cathodes, utilization of a suitable current collector is very important to obtain accurate results. The current collectors used at the cathode side must exhibit high electronic conductivity under oxidizing atmospheres and at high temperatures (i.e. 500-750 °C). In addition, they must be chemically stable and compatible with adjacent components while possessing sufficient porosity to allow for effective gas delivery to the electrochemically active sites. These stringent requirements are met by only a handful of noble metals such as; gold (Au), platinum (Pt) and silver (Ag). All of these metals exhibit high electronic conductivity at high temperatures (Au 10.6×10^4 Scm^{-1}, Pt 2.6×10^4 Scm^{-1} and Ag 14.6×10^4 Scm^{-1} at 800 °C, Zhu and Ghezel-Ayagh, 2017). However, among these metals, Ag is by far the most cost-effective one, i.e., its per ounce price is ca. 50 times lower than that of Au and Pt (West and Manthiram, 2015).

Ag current collectors are usually applied onto the SOFC cathode by screen-printing or brush painting an ink containing the Ag particles followed by a heat treatment to ensure bonding among the Ag particles and provide good attachment of the current collector to the cathode surface (Gong et al., 2012; Guo et al., 2011; Sarikaya et al., 2012a). Upon the preparation of Ag inks, addition of glassy phase particles (frit) has been a frequently encountered approach to ensure a stronger bonding to the substrate (Rane et al., 2004). However, the effect of the presence of frit on the accuracy of the electrochemical impedance spectroscopy measurements of SOFC cathodes remains unknown. Hence, in this study, the effect of the presence of frit on the microstructure of the fired Ag current collector layer and the measured electrochemical performance of the cathode is investigated.

2. Materials and Methods

To understand the effect of frit content, which is usually present in the Ag current collector inks for good adhesion, on the measured cathode performance, symmetrical half-cells, based on thick yttria stabilized zirconia (YSZ) electrolyte substrates were prepared. To prepare the YSZ electrolyte substrates YSZ powders (Tosoh, Japan) were consolidated into a disk shape by die pressing and then a tighter packing was achieved by cold isostatic pressing under 200 MPa. The obtained discs were sintered at 1400 °C for 2 hours in air to achieve dense ceramics.

The $La_{0.6}Sr_{0.4}FeO_3$ (LSF) cathodes were formed on each side of the YSZ substrates to achieve symmetrical with the LSF/YSZ/LSF configuration. This was realized by spin coating a polymeric LSF precursor onto the YSZ ceramics. To prepare the polymeric LSF precursor solutions, strontium nitrate ($Sr(NO_3)_2$, ≥ 99%, Sigma-Aldrich), lanthanum (III) nitrate hexahydrate ($La(NO_3)_3.6H_2O$, ≥ 99%, Fluka) and iron(III) nitrate nonahydrate ($Fe(NO_3)_3.9H_2O$, ≥ 99%, Sigma-Aldrich) salts were dissolved in distilled water. Ethylene glycol was added to the resultant solution, which was then stirred at 80 °C until whole water had evaporated. Finally, 2-butoxyethanol was added to the solution for improved wetting of the YSZ substrate during the coating process. The spin-coating process was performed at a rotation speed of 3000 rpm. The achieved LSF/YSZ/LSF symmetrical half-cells were sintered at 700 °C for 3 hours to achieve crystallized thin film cathodes.

Both sides of the LSF/YSZ/LSF symmetrical half-cells were coated either with frit-free or frit containing Ag inks, denoted as Ag-ff and Ag-f respectively. The frit-free Ag ink was prepared in our laboratories by mixing Ag powder (Nanokar, Turkey, 99.9%) with α-terpineol (Alfa-Aesar, 96%) and 2-butoxyethanol (Acros Organics, 99%) in a 22:4:1 weight ratio using mortar and pestle. The frit containing Ag ink was purchased commercially (Arıteks, Turkey). The Ag current collector inks were deposited by brush painting, followed by heat treatment at 600 °C for 3 hours in air.

The microstructural and elemental analyses of the Ag-ff and Ag-f current collector layers were performed by scanning electron microscopy/energy dispersive x-ray spectroscopy (Philips XL30 SEFG SEM). The electrochemical performance of the Ag-f/LSF/YSZ/LSF/Ag-f and Ag-ff/LSF/YSZ/LSF/Ag-ff symmetrical half-cells were investigated by electrochemical impedance spectroscopy measurements performed using a Biologic-SP150 potentiostat/galvanostat/impedance analyzer, at 450-700 °C, in stagnant air.

3. Results and Discussion

Scanning electron microscopy (SEM) analyses performed on the current collectors fabricated from frit containing (Ag-f) and frit-free (Ag-ff) Ag reveal the effect of the frit content on the microstructure of the current collectors (Figure 1). Figures 1a and b show the top surface and cross-sectional views of the Ag-ff layer respectively after sintering at 600 °C for 3 hours, in air. The average particle size of Ag-ff layer is ca. 3 μm and has a porous structure that should allow facile transport of the oxygen gas to the electrocatalytically active $La_{0.6}Sr_{0.4}FeO_3$ (LSF) surface. Using image analysis by ImageJ, the porosity of the Ag-ff layer is determined as 21%.

Figures 1c and 1d depict the surface and cross-sectional SEM views of the Ag-f layer. The top surface image reveals a pore-free microstructure consisting of two interconnected phases with distinct morphologies (Figure 1c). One of these phases has a facetted morphology suggesting a crystalline nature, while the other exhibits a continuous and featureless morphology, suggesting a glassy phase (Figure 1c). The cross-sectional SEM image of the Ag-f layer shows only a few large pores that are not interconnected, and hence would not contribute to the gas transport (Figure 1d).

Table I provides the atomic and weight ratios of the elements determined by energy dispersive x-ray spectroscopy analyses performed in areas representative of the Ag-ff and Ag-f current collectors (Areas 1 and 2 in Figures 1a and c respectively), in addition to those performed in areas consisting solely of the faceted and featureless phases (Areas 3 and 4 respectively). Here, for facile comparison of the elemental ratios, the signals corresponding to oxygen are omitted. Area 1 is determined to consist solely of Ag, with small intensities of Y and Zr signals also reaching the detector from the YSZ substrate, through the porous current collector (Table I). Area 2 represents the general surface of the Ag-f current collector and along with Ag, signals belonging to Zn, Al, Si and Ba elements, the oxides of which constitute the glassy frit phase, are obtained (Table I). The faceted phase in the Ag-f current collector (Area 3) evidently is Ag, while the featureless phase (Area 4) consists mainly of the frit content in the commercial Ag-f ink (Table I).

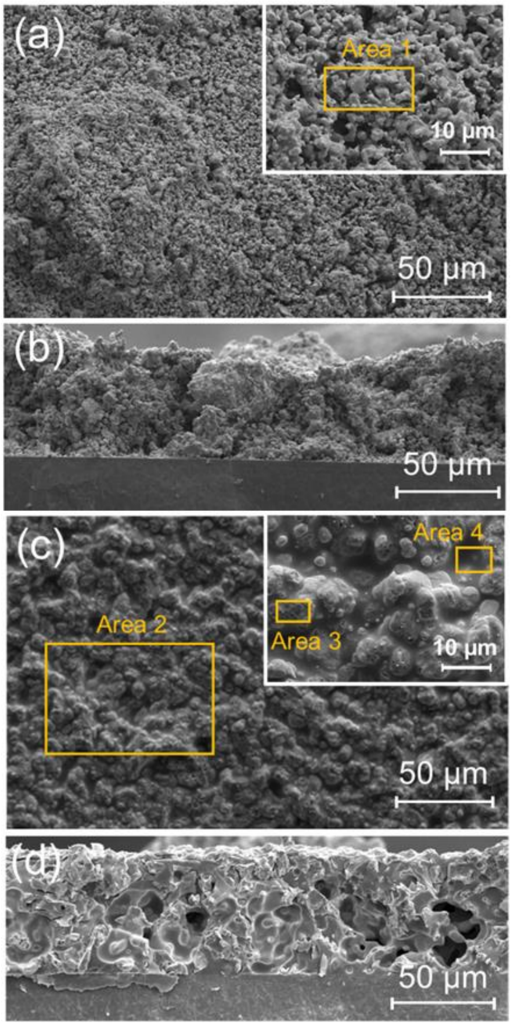

Figure 1. Scanning electron microscopy images of a) the top-down b) the fracture surfaces of Ag-ff current collectors, c) top down and d) fracture surfaces of Ag-f current collectors after heat treatment at 600 °C for 3 hours, in air.

Table 1. Relative amounts of elements obtained from the energy dispersive x-ray spectroscopy analysis performed on the four areas at the surfaces of Ag-f and Ag-ff current collector layers shown in Figure 1.

Elements	Atomic % in Area 1	Atomic % in Area 2	Atomic % in Area 3	Atomic % in Area 4
Ag	97.28	18.29	90.91	5.54
Zn	………	43.82	9.09	77.65
Al	………	6.22	………	1.73
Si	………	29.77	………	6.23
Ba	………	1.90	………	8.49
Y	1.09	………	………	………
Zr	0.92	………	………	………

The current collector performance of Ag-f and Ag-ff layers are investigated via electrochemical impedance spectroscopy (EIS) measurements of symmetrical half-cells with yttria stabilized zirconia (YSZ) electrolytes and $La_{0.6}Sr_{0.4}FeO_3$ (LSF) thin film electrodes (cell configuration: current collector/LSF/YSZ/LSF/current collector), in stagnant air. EIS measurements of symmetrical half-cells carried out under open circuit conditions (0 V) and an amplitude of 10 mV from 0.5 MHz to 0.2 Hz. Figures 2a-c shows the Nyquist plots obtained from the symmetrical half-cells with Ag-f or Ag-ff current collectors at 700, 641 and 588 °C respectively, in air. For a facile comparison of the electrochemical response in the two types of samples, the impedance data are normalized to unit area by multiplying both the imaginary and real coordinates by the geometric electrode area (Figure 2a-c). Here, in general, the impedance spectra are interpreted as consisting of two parts; i) the high frequency intercept corresponding to the area specific ohmic resistance (denoted as ASR1) and ii) the distance between the low frequency and the high frequency intercepts (ASR2), referred to as the "polarization resistance" (Figure 2a inset). ASR1 comprises of area specific resistance contributions originating from the resistance to the ionic transport through the YSZ electrolyte + the resistivity of the LSF thin film electrons + any current collector resistances. Since LSF exhibits a very high electronic conductivity under the present experimental conditions, (ca. 100 Scm^{-1} at 700 °C, in air, Patrakeev et al., 2015) and is fabricated in the form of thin films in the present case (i.e., thickness< 1 µm) its contribution to the ohmic resistance is negligible here. ASR2 (the polarization resistance) refers to the inverse of the oxygen reduction/oxygen evolution reaction (ORR/OER) activity at the two LSF electrodes, i.e., polarization resistance per electrode is the half of ASR2. At all temperatures, the impedance arc obtained from the symmetrical half-cells using Ag-f current collectors starts at higher ASR1 values than those using ASR-ff current collectors (Figures 2a-c). In addition, very large ASR2 values (in the range of hundreds of Ωcm^2) are obtained at all temperatures when Ag-f is used (Figures 2a-c). On the other hand, quite acceptable electrode polarization resistances, e.g., 0.5 Ωcm^2 at 700 °C (Figure 2a), are obtained when Ag-ff current collectors are employed.

For a clear interpretation of the impedance responses obtained from symmetrical half-cells with Ag-f and Ag-ff current collectors, the ohmic and polarization responses are analyzed separately. Figure 3a shows the temperature dependence of the ohmic resistance obtained from the symmetrical half-cells employing Ag current collectors with and without frit content. As expected, area specific resistance (ASR1) follows an Arrhenius-type behavior in both cases with similar slopes. However, the ohmic resistances obtained from the symmetrical half-cells employing Ag-f current collectors are approximately 3-4 times those employing Ag-ff current collectors. The higher ohmic resistances observed in the case of Ag-f current collectors is considered to be directly related to the composition of the ink this current collector was prepared from. The significant amount of glassy phase in the Ag-f current collectors (18.29 at.% Ag in Area 2, Table I) results in a smaller interfacial contact area between the Ag particles and LSF thin film cathode than that exists in the case of Ag-ff current collectors causes higher ASR1 values.

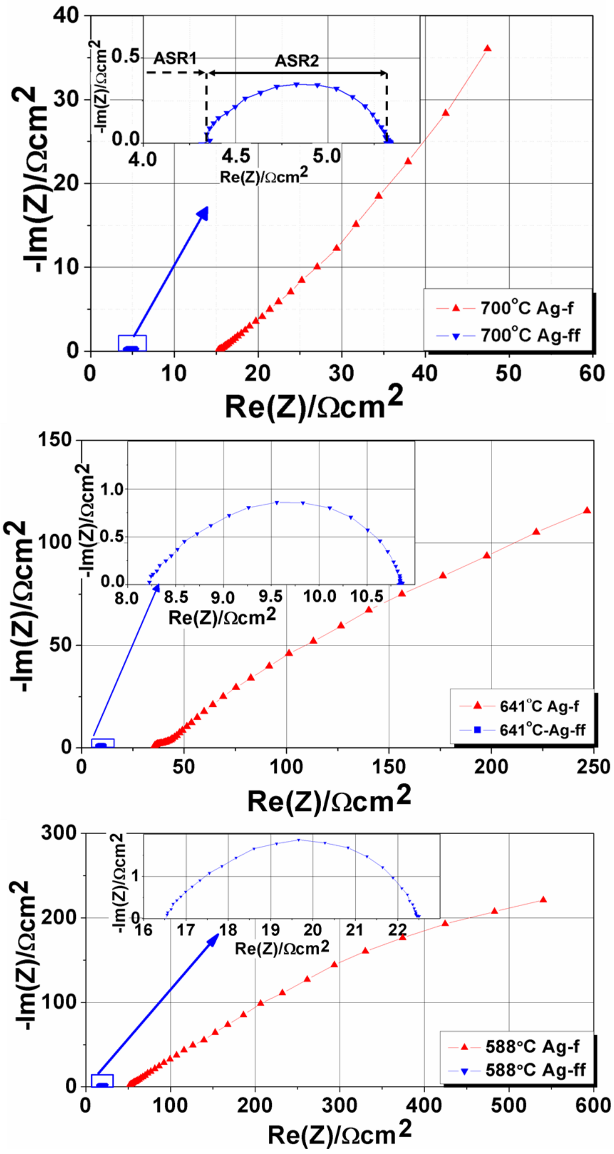

Figure 2. Nyquist plots constructed from the electrochemical impedance spectroscopy measurements performed on Ag-f/LSF/YSZ/LSF/Ag-f and Ag-ff/LSF/YSZ/LSF/Ag-ff symmetrical half-cells, at a) 700, b) 641 and c) 588 °C.

To determine whether ASR1 obtained from the Ag-ff current collector is at an acceptable value, the electrical conductivity of the YSZ electrolyte is calculated using Eq. (1) and its temperature dependence is compared to the data from the literature (Figure 3b). In Eq. (1), σ and L refer to the electrical conductivity and the electrolyte thickness respectively.

$$\sigma = \frac{L}{(ASR1)} \qquad (1)$$

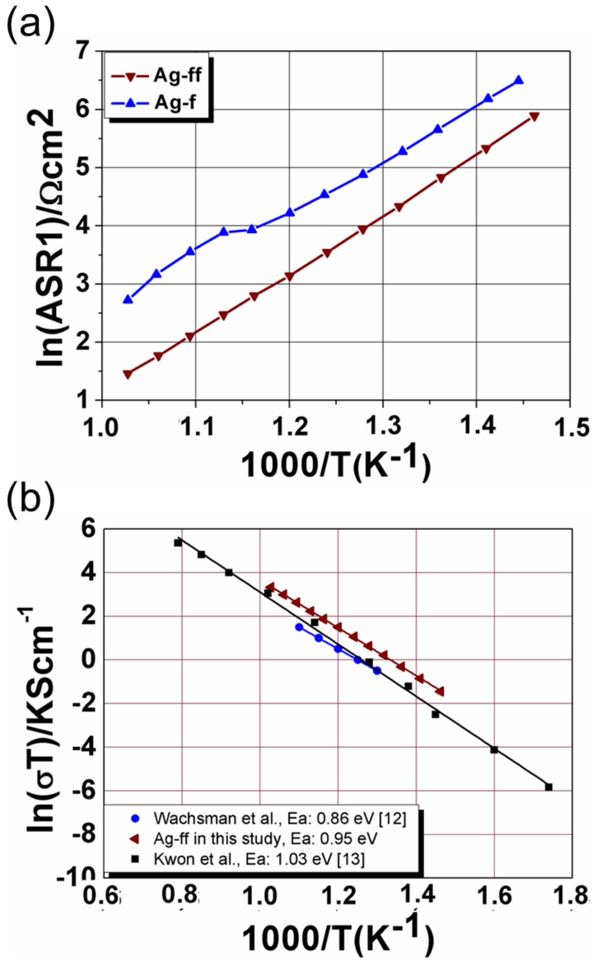

Figure 3. Temperature dependence of a) the ohmic resistance obtained from the electrochemical impedance spectroscopy measurements of Ag-f/LSF/YSZ/LSF/Ag-f and Ag-ff/LSF/YSZ/LSF/Ag-ff symmetrical half-cells and b) the electrical conductivity of the YSZ electrolytes calculated from the ohmic resistance of the Ag-ff/LSF/YSZ/LSF/Ag-ff symmetrical half-cell. The electrical conductivity values from the literature are also included in the latter for comparison (Wachsman et al., 2014; Kwon and Choi, 2006; Kosacki et al., 2005).

The electrical conductivity of YSZ measured in the present study using symmetrical half-cells with LSF cathodes and Ag-ff current collectors is at an acceptable value, e.g., 0.066 Scm^{-1} at 700 °C. Over a wide temperature range, the electrical conductivity values obtained here for YSZ using the frit-free Ag current collector lie even slightly higher in comparison to the data obtained by E. Wachsman et al. (2014) and Kwon and Choi (2006). The activation energy for the electrical conductivity is determined as 0.95 eV, agreeing well with the values reported in the literature for the oxygen ion transport through the YSZ lattice (Kosacki et al., 2005) and those reported by Wachsman et al. (2014) and Kwon and Choi (2006).

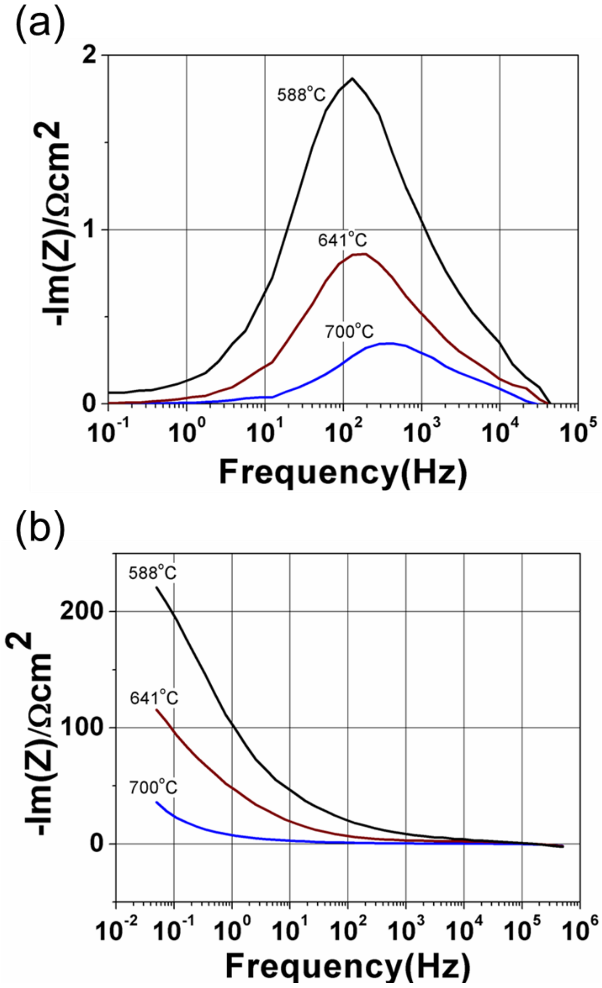

Figure 4. Bode plots constructed from the electrochemical impedance spectroscopy measurements performed on a) Ag-ff/LSF/YSZ/LSF/Ag-ff and b) Ag-f/LSF/YSZ/LSF/Ag-f symmetrical half-cells, at 700, 641 and 588 °C.

Another important criterion that determines the suitability of the cathode current collector is the cathode polarization resistance that is obtained upon its use. The Nyquist plots given in Figure 2 suggest that the Ag-ff current collector allows the achievement of acceptable cathode polarization resistances, while Ag-f does not. However, a more detailed analysis is required to understand what makes the Ag-f unsuitable for obtaining low cathode polarization resistances. For this purpose, Bode diagrams are constructed from the impedance responses of the symmetrical half-cells employing Ag-f and Ag-ff current collectors (Figure 4). The EIS response of the symmetrical half-cells using Ag-ff current collectors obtained at 588 °C exhibit a single peak at the 10^2 Hz, which decreases in magnitude and increases in frequency with increasing temperature (Figure 4a). This behavior points to a temperature dependent electrochemical process and suggests that there is sufficient access of oxygen gas to the LSF thin film cathode. On the other hand, Figure 4b shows that the single peak in this case appears at frequencies below

10^{-2} Hz, which is out of the measurement range of our device. It is also seen that with increasing temperature, the summit frequency remains out of range, but the magnitude of the imaginary part of the impedance decreases (Figure 4b). It may be argued that the dense microstructure (shown in Figure 1c) and the low frequency nature of the peak observed in the Bode plot (Figure 4b) corresponds to limited oxygen gas diffusion to the LSF surface, i.e., concentration polarization dominates the EIS response. However, concentration polarization is characterized by a weak dependence on temperature (Primdahl and Mogensen, 1999), whereas a clear decrease in the imaginary part of the impedance is observed here (Figure 4b).

An alternative explanation to the extremely poor electrochemical performance observed in the case of Ag-f current collectors is again connected to the dense microstructure originating from the glassy phase content, shown in Figure 1c. It is well-known that glassy pastes have been employed as gas sealants in SOFC stacks to prevent the intermixing of the fuel and oxygen gases (Fergus, 2005). Therefore, it is reasonable to assume that the glassy phase present in the Ag-f current collector completely blocks the surface of the LSF (instead of partially limiting gas transport there) and renders this layer inactive for the ORR/OER, as schematically depicted in Figure 5a. In this case, since no electrocatalytic activity is expected from the glassy phase, only the surfaces of Ag particles at the outer surface of the Ag-f current collector remain as the available sites for oxygen adsorption and reduction (Figure 5a). The extremely small amount of Ag surface that the Ag-f current collector exposes for oxygen adsorption and reduction is one factor that causes high polarization resistances at low frequencies. The other factor in the proposed scenario is that the percolated Ag network acts as the sole oxygen ion conducting path (Sarikaya et al, 2012b; Kontoulis and Steele, 1991), which is a long one (Ag-f layer is ca. 50 µm thick). Further experiments involving EIS measurements on symmetrical half-cells employing Ag-f current collectors with different thicknesses are required to determine which process (oxygen adsorption/reduction at the surface or diffusion through the Ag lattice) dominates the EIS response.

On the other hand, when no glassy phase is present in the Ag current collector and when this layer is porous, the oxygen gas is facilely transported to the active surfaces of the LSF particles of the thin film cathode where fast ORR/OER takes place.

5. Summary

A common practice to ensure adhesion of Ag current collector inks onto the surfaces of the solid oxide fuel cell cathodes is the addition of a glassy phase, which may undergo a glass transition at the operating temperatures of 500-700 °C. In this study, the effects of frit addition on the measured electrochemical performance of $La_{0.6}Sr_{0.4}FeO_3$ (LSF) cathodes has been investigated. The microstructure and electrochemical performance of two types of symmetrical half-cells; one utilizing frit-free, the other frit containing Ag current collectors were compared. The symmetrical half-cell employing current collector without frit exhibits a very acceptable cathode polarization and ohmic resistances. On the other hand, the half-cell with the frit containing Ag current collector showed slightly higher ohmic resistances and extremely large cathode polarization resistances. This was explained by the extremely dense microstructure of the frit containing Ag current collector layer i) reducing the Ag-LSF interfacial contact area and ii) blocking the electrocatalytic LSF surface, thus causing poor current collection and low electrochemical performance respectively.

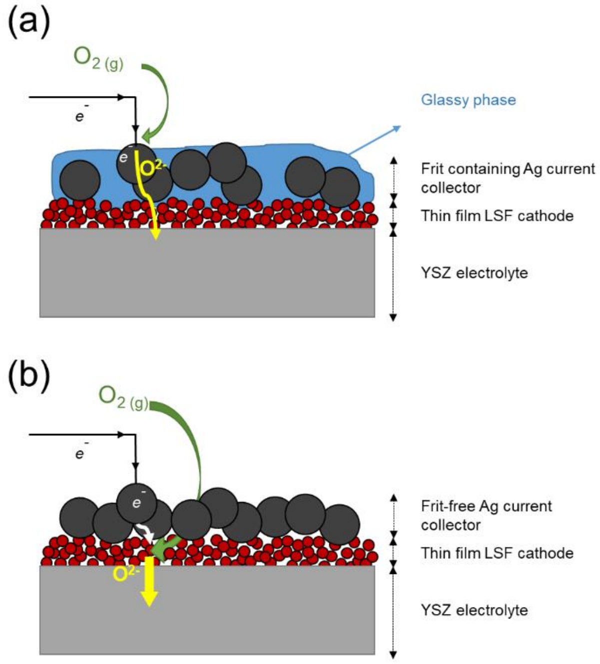

Figure 5. Schematic representation of the oxygen reduction pathway when a) frit containing Ag (Ag-f) and b) frit-free Ag (Ag-ff) current collector inks are used on LSF thin film cathodes.

Acknowledgements

We gratefully acknowledge Mr. Ahmet Nazım for his help operating the SEM and Gebze Technical University for partially funding this work through a scientific research project (Project number: 2017-A-50).

Conflict of Interest

No conflict of interest was declared by the authors.

References

Chen, X., Tao, Z., Hou, G., Xu, N., Zhang, Q., 2015. $La_{0.7}Sr_{0.3}FeO_{3-\delta}$ composite cathode enhanced by $Sm_{0.5}Sr_{0.5}CoO_{3-\delta}$ impregnation for proton conducting SOFCs. Electrochim. Acta. 165, 142–148.

Fergus, J. W., 2005. Sealants for solid oxide fuel cells. J. Power Sources. 147, 46–57.

Gong, Y., Qin, C., Huang, K., 2012. Can Silver Be a Reliable Current Collector for Electrochemical Tests? ECS Electrochemistry Letters. 2, F4-F7.

Guo, Y. M., Zhou, Y. B., Chen, D. J., Shi, H. G., Ran, R., Shao, Z.P., 2011. Significant impact of the current collection material and method on the performance of $Ba_{0.5}Sr_{0.5}Co_{0.8}Fe_{0.2}O_{3-\delta}$ electrodes in solid oxide fuel cells. J. Power Sources. 196, 5511-5519.

Kontoulis, I., Steele, B.C.H. 1991. Determination of oxygen diffusion in solid Ag by an electrochemical technique. Solid State Ionics. 47, 317-324.

Kosacki, I., Rouleau, C. M., Becher, P. F., Bentley, J., Lowndes, D. H., 2005. Nanoscale effects on the ionic conductivity in highly textured YSZ thin films. Solid State Ionics. 176, 1319 – 1326.

Kwon, O.H., Choi, G.M., 2006. Electrical conductivity of thick film YSZ. Solid State Ionics. 177, 3057-3062.

Li, M., Wang, Y., Wang, Y., Chen, F., Xia, C., 2014. Bismuth Doped Lanthanum Ferrite Perovskites as Novel Cathodes for Intermediate-Temperature Solid Oxide Fuel Cells. ACS Appl. Mater. Interfaces. 6, 11286–11294.

Lyskov, N. V., Kolchina, L. M., Galin, M. Z., Mazo, G. N., 2018. Development of lanthanum-doped praseodymium cuprates as cathode materials for intermediate-temperature solid oxide fuel cells. Solid State Ionics. 319; 156-161.

Patrakeev, M. V., Leonidov, I. A., Kozhevnikov, V. L., Poeppelmeier, K.R., 2005. p-Type electron transport in $La_{1-x}Sr_xFeO_{3-\delta}$ at high temperatures J. Solid State Chem. 178; 921–927.

Primdahl, S., Mogensen, M. 1999. Gas Diffusion Impedance in Characterization of Solid Oxide Fuel Cell Anodes. J. Electrochem. Soc. 146; 2827-2833.

Rane, S. B., Seth, T., Phatak, G. J., Amalnerkar, D. P., 2004. Effect of inorganic binders on the properties of silver thick films. J. Mater. Sci. Mater. Electron. 15, 103-106.

Sarikaya, A., Petrovsky, V., Dogan, F. Development of a silver based stable current collector for solid oxide fuel cell cathodes in: proceedings of the materials research society fall meeting 2011, Boston, United States, November 28-December 2, vol. 1385, Cambridge University Press, 2012, p. c07.

Sarikaya, A., Petrovsky, V., Dogan, F., 2012. Silver composites as highly stable cathode current collectors for solid oxide fuel cells. J. Mater. Res. 27, 2024-2029.

Tatko, M., Mosiałek, M., Dudek, M., Nowak, P., Kędra, A., Bielańska E., 2015. Composite cathode materials $Sm_{0.5}Sr_{0.5}CoO_3$–$La_{0.6}Sr_{0.4}FeO_3$for solid oxide fuel cells. Solid State Ionics. 271, 103–108.

Wachsman, E., Ishihara, T., Kilner, J., 2014. Low-temperature solid-oxide fuel cells. MRS Bulletin. 39, 773-779.

West, M., Manthiram, A., 2015. Synthesis of 3-dimensional silver networks and their application in solid oxide fuel cells. Int. J. Hydrogen Energy. 40, 4234-4240.

Zhu, J.H., Ghezel-Ayagh, H., 2017. Cathode-side electrical contact and contact materials for solid oxide fuel cell stacking: A review. Int. J. Hydrogen Energy. 42, 24278-24300